

Article

The Lewis Pair Polymerization of Lactones Using Metal Halides and *N*-Heterocyclic Olefins: Theoretical Insights

Jan Meisner¹, Johannes Karwounopoulos¹ , Patrick Walther² , Johannes Kästner¹  and Stefan Naumann^{2,*} 

¹ Institute of Theoretical Chemistry, University of Stuttgart, Pfaffenwaldring 55, D-70569 Stuttgart, Germany; meisner@theochem.uni-stuttgart.de (J.M.); johannes.karwou@googlemail.com (J.K.); kaestner@theochem.uni-stuttgart.de (J.K.)

² Institute of Polymer Chemistry, University of Stuttgart, Pfaffenwaldring 55, D-70569 Stuttgart, Germany; patrick.walther@ipoc.uni-stuttgart.de

* Correspondence: stefan.naumann@ipoc.uni-stuttgart.de, Tel.: +49-0711-685-64090

Received: 15 January 2018; Accepted: 12 February 2018; Published: 15 February 2018

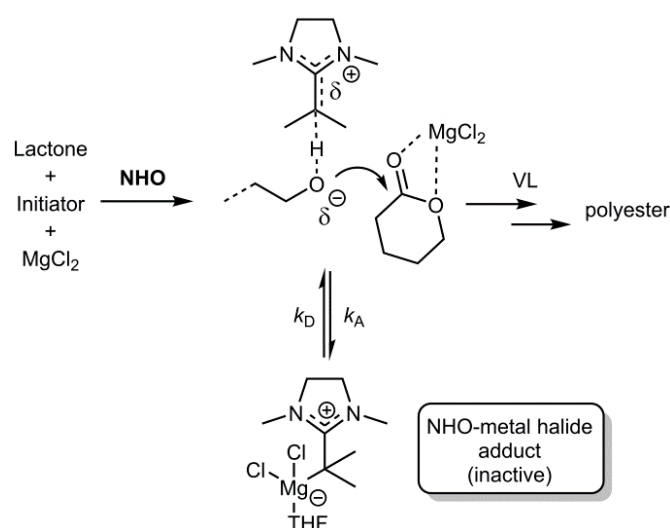
Abstract: Lewis pair polymerization employing *N*-Heterocyclic olefins (NHOs) and simple metal halides as co-catalysts has emerged as a useful tool to polymerize diverse lactones. To elucidate some of the mechanistic aspects that remain unclear to date and to better understand the impact of the metal species, computational methods have been applied. Several key aspects have been considered: (1) the formation of NHO-metal halide adducts has been evaluated for eight different NHOs and three different Lewis acids, (2) the coordination of four lactones to MgCl₂ was studied and (3) the deprotonation of an initiator (butanol) was investigated in the presence and absence of metal halide for one specific Lewis pair. It was found that the propensity for adduct formation can be influenced, perhaps even designed, by varying both organic and metallic components. Apart from the NHO backbone, the substituents on the exocyclic, olefinic carbon have emerged as interesting tuning site. The tendency to form adducts is ZnCl₂ > MgCl₂ > LiCl. If lactones coordinate to MgCl₂, the most likely binding mode is via the carbonyl oxygen. A chelating coordination cannot be ruled out and seems to gain importance upon increasing ring-size of the lactone. For a representative NHO, it is demonstrated that in a metal-free setting an initiating alcohol cannot be deprotonated, while in the presence of MgCl₂ the same process is exothermic with a low barrier.

Keywords: Lewis pairs; polyesters; *N*-heterocyclic olefins; density functional theory

1. Introduction

Among the many approaches towards polymerization-active Lewis pairs (LPs) [1–9], the combination of commercially available metal halides (MX_n) and readily accessible organobase catalysts (OBCs) provides very simple, yet surprisingly powerful access to LP catalysts for lactone polymerization [10–12]. Thereby, it is assumed that the Lewis acid (MgCl₂, ZnCl₂, LiCl ...) coordinates to the monomer, accepting electron density and thus increases the polarization of the carbonyl group (Scheme 1). This facilitates attack by an (organic) nucleophile (i.e., an alcohol initiator activated by the applied OBC) and subsequent ring-opening. This has repeatedly been described to result in increased polymerization rates, including cases where it is only the cooperative interaction between Lewis base and Lewis acid which engenders reactivity in the catalytic setup—quite frequently, the individual components are fully polymerization-inactive on their own [2,4,10–12]. Our group has recently expanded on several other key aspects of this chemistry [10–12]. For one, it was demonstrated that reactivity and selectivity can be decoupled for many examples of MX_n/OBC Lewis

pair polymerization of lactones. This means that higher polymerization rates are not simultaneously accompanied by increased transesterification, the major side reaction responsible for broad molecular weight distributions and limited molecular weights. This beneficial behavior was attributed to the ability of the activating Lewis acid to differentiate between the polymer chain and the cyclic monomer. Moreover, the inherent adaptability of this setup (both components can be exchanged independently) has enabled a broad applicability: lactone monomers as different as γ -butyrolactone (GBL, Figure 1), δ -valerolactone (VL), ϵ -caprolactone (CL) or pentadecalactone (PDL) were successfully homo- or copolymerized. Crucially, the choice of activating Lewis acid not only modulates the polymerization rates, but is also a convenient tool to manipulate the copolymerization parameters. The preparation of aliphatic polyester with different compositions from the same 1:1 comonomer feed can thus be realized; the incorporation of significant amounts of GBL was also possible [11,12]. This effect was proposed to originate from a certain degree of monomer selectivity displayed by the activating Lewis acid. Different metal halides will activate different lactone monomers to a varying extent because they differ in parameters such as steric hindrance, ion radii, monomer-metal complex stability or the O–C–O angle of the lactone.



Scheme 1. Simplified reaction mechanism for the cooperative activation of initiators/propagating chain ends and monomers in the *N*-Heterocyclic olefin (NHO)/metal halide Lewis pair (LP)-catalyzed polymerization of lactones. The adduct is assumed to be inactive.

During these studies, *N*-heterocyclic olefins (NHOs) have been identified as especially suited for these applications. NHOs are reactive OBCs on account of their highly polarized double bond (Figure 1) [13–18]; the high electron density on the exocyclic carbon renders it nucleophilic [19] and a strong Brønsted-base [20]. Additionally, this polarization can be readily tuned and synthesis is usually limited to few and simple steps [21–23]. Owing to their steadily increasing popularity, NHOs and their structural and catalytic properties have also been the focus of other detailed theoretical studies [24–31].

In view of the high performance and promising prospects of this type of Lewis pair polymerization, a better understanding of the underlying mechanisms is much desired. A rewarding long-term goal would be the ability to design the MX_n /OBC pairs so as to tailor the resulting polymer material with regard to architecture (random, gradient, block-like) and composition (comonomer content), arriving at a polyester with rationally pre-determined properties. However, presently, systematic investigations on this subject are missing and even very basic questions remain unresolved. For example, it is not clear how the Lewis acid actually coordinates with the lactone; three different modes can be envisioned

(Figure 2). The influence of the Lewis acid on initiation and propagation is equally diffuse as yet, and coherently the origin of the experimentally observed monomer selectivity is still elusive.

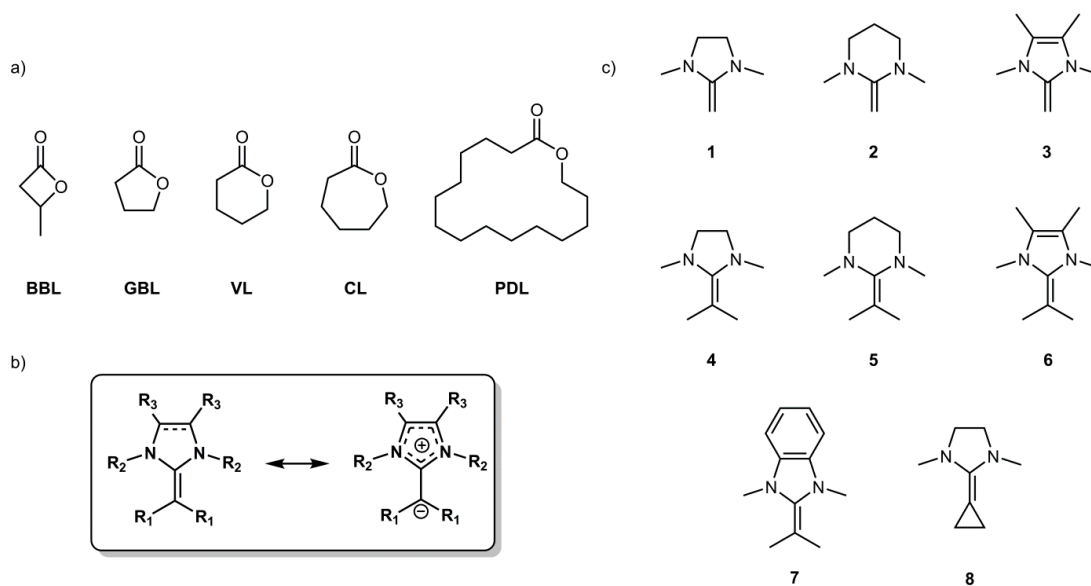


Figure 1. (a) Different lactones that have been polymerized by NHO/metal halide LPs; (b) mesomeric structure emphasizing the polarized character of the NHO double bond; (c) range of NHOs considered in this work. BBL: β-butyrolactone; GBL: γ-butyrolactone; VL: δ-valerolactone; CL: ε-caprolactone; PDL: pentadecalactone.

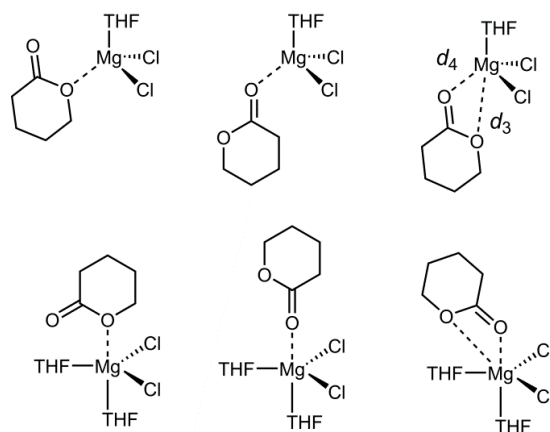


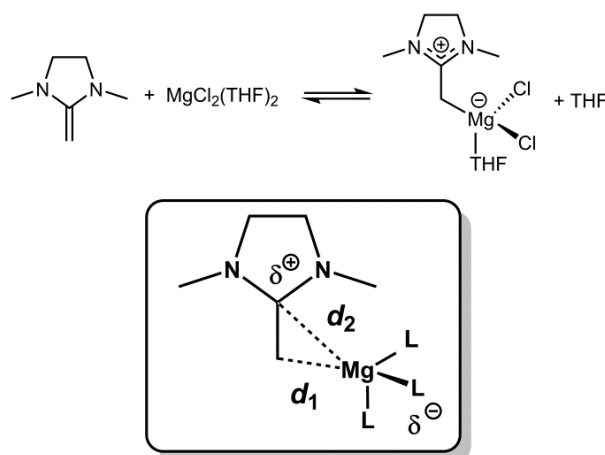
Figure 2. Investigated types of lactone-ligated magnesium complexes. Top: Tetrahedral geometry; Bottom: Trigonal-bipyramidal coordination. From left to right: endocyclic activation, carbonyl activation and chelating activation.

While this work does not attempt to describe a comprehensive mechanistic scenario for ring-opening polymerization using NHO/metal halide LPs, it is intended to elucidate some central aspects of the discussed polymerization pathways by way of density functional theory (DFT) calculations. We have included several different metal halides in this study (MgCl₂, ZnCl₂, LiCl), as well as a representative number of various NHO structures (1–8, Figure 1) and lactone monomers. The issues investigated in the following are (i) the stability of NHO/MX_n adducts; (ii) the lactone/MX_n coordination (mode) and (iii) finally the proton transfer from the initiator to the NHO in the presence of a Lewis acid, detailed for one example.

2. Results

2.1. Lewis Acid—Lewis Base Adducts

As a first step, NHO-adduct formation was investigated. Since the currently proposed polymerization mechanisms [11,12] are based on the assumption of a free NHO acting in cooperation with a free, i.e., non-complexed, Lewis acid, a sufficient lability of potential NHO-metal complexes in a given LP polymerization system must be ensured. The formation of too stable adducts would quench any polymerization activity; on the other hand, the choice of a too weakly coordinating metal ion will also impair its ability to activate lactones for ring-opening—an issue that has been identified as central in several polymerization systems employing *N*-heterocyclic carbenes (NHCs) or NHOs [4,10–12,32]. Thus, in order to achieve a better understanding of this required balance, the affinity of eight structurally different NHOs (1–8, Figure 1) to bind to each of the Lewis acids MgCl₂, ZnCl₂ and LiCl was investigated. Adduct geometries were optimized and the Gibbs Free Energy of the reaction (ΔG_R) as shown in Scheme 2 was compared. Furthermore, the metal–C bond distances were investigated to obtain additional insight into the strength of the interaction. It should be noted that for the considered reaction, the NHO substitutes a tetrahydrofuran (THF) ligand; the generated complex is neutral, yet a charge separation takes place, locating the positive charge on the NHO ligand. A tetrahedral complex geometry was employed and it was assumed that the metal–Cl bond will resist substitution. THF is a typical solvent for lactone polymerization and the existence of such tetrahedral structures has been demonstrated for closely related NHC complexes such as ZnCl₂(SIMes)(THF) [4]. The results for MgCl₂, ZnCl₂, and LiCl are shown in Tables 1–3, respectively.



Scheme 2. Investigated formation of NHO/Lewis acid adducts and definition of d_1/d_2 .

Table 1. Properties of the MgCl₂(NHO)(THF) complexes.

NHO	ΔG_R (kJ/mol)	d_1 (Å)	d_2 (Å)
1	−9.0	2.26	2.96
2	−17.1	2.25	3.04
3	−32.3	2.24	3.02
4	+20.0	2.31	2.90
5	+20.9	2.36	2.93
6	−9.6	2.27	2.99
7	+12.4	2.34	2.90
8	−21.8	2.21	3.09

Table 2. Properties of the ZnCl₂(NHO)(THF) complexes.

NHO	ΔG_R (kJ/mol)	d_1 (Å)	d_2 (Å)
1	−26.6	2.09	2.88
2	−30.7	2.08	2.89
3	−53.4	2.07	2.95
4	+7.6	2.13	2.85
5	+11.0	2.16	2.84
6	−25.3	2.10	2.85
7	+2.3	2.15	2.82
8	−44.1	2.06	2.92

Table 3. Properties of the LiCl(NHO)(THF)₂ complexes.

NHO	ΔG_R (kJ/mol)	d_1 (Å)	d_2 (Å)
1	+15.2	2.38	2.81
2	+11.9	2.36	2.86
3	+12.9	2.33	3.00
4	+29.9	3.00	2.94
5	+17.6	2.83	3.12
6	+14.2	2.54	2.77
7	+27.2	2.68	2.92
8	+10.0	2.31	2.79

From these data, a number of conclusions can be drawn. As a consequence of the strong polarization of the olefinic double bond, the NHOs coordinate preferably with the exocyclic carbon atom to Mg²⁺ or Zn²⁺ (η^1 bonding). This is in accordance with experimental findings; end-on rather than side-on coordination is typical for NHOs and has been described for a range of different metal complexes [13,17,18,33]. Hence, the parameters d_1 and d_2 , defined as the distances of the metal to the exo- and endocyclic olefinic carbon (Scheme 2), can serve as a direct probe for any degree of side-on coordination. Interestingly, a direct comparison immediately reveals differences in this respect for the magnesium-, zinc- and lithium-complexes. While the MgCl₂ adduct (Table 1) displays a clear preference for end-on binding, this property is even more pronounced for the ZnCl₂-based analogue (Table 2), where the corresponding Δd is largest although the average bonding distances d_1 and d_2 are even somewhat smaller than found for the series of MgCl₂-complexes. In contrast, the LiCl series displays larger d values, implying a rather weak coordination. Also, the asymmetry between d_1 and d_2 is milder and in some cases the lithium takes up a virtually equidistant position relative to the two olefinic carbons. This effect is obviously influenced by the chemical structure of the NHO and most pronounced for 4, which may be explained by the relatively low double bond-polarization in this molecule (see below). The increasing tendency to form end-on coordinated adducts in the sequence Li⁺ < Mg²⁺ < Zn²⁺ as described by d_1/d_2 is coherently mirrored by the Gibbs Free Energy of the reaction, which shows the adduct formation to be increasingly exothermic in the same sequence.

This is true for the full range of all eight investigated NHOs, suggesting that for any given system the proportion of free NHO is highest for LiCl and lowest for ZnCl₂ (for the latter, the reaction enthalpy is by 15 kJ/mol smaller on average than found for MgCl₂). The stronger tendency of ZnCl₂ than MgCl₂ to bind to the investigated NHOs is also expressed in shorter Zn-C bond lengths (compare Tables 1 and 2, on average 0.15 Å shorter), in spite of the very similar ionic radii of Mg²⁺ and Zn²⁺. The binding to Li⁺ is unfavorable compared to the binding affinity to Mg²⁺ by up to 45 kJ/mol and compared to ZnCl₂ by up to 65 kJ/mol, depending on the NHO. In this context it should be noted that the same tendency seems to apply for analogous NHC complexes (MgCl₂/ZnCl₂) [4], supporting the findings in this work.

The chemical structure of the NHO significantly influences the reaction energies, allowing for some instructive comparisons. The results are more clearly cut for the zinc- and magnesium

analogues—not surprisingly, since here a proper bond is formed—while for the LiCl complexes the weak interaction equalizes the reaction energies. Thus, for compounds 1–3, a series of NHOs with no further substituent on the exocyclic carbon (C=CH₂ moiety), the bonding propensity increases on going from 1 over 2 to 3. This nicely matches literature reports, which indicate that a six-membered, tetrahydropyrimidine-based structure such as 2 should be somewhat more reactive than 1 [34], while imidazole derivatives (3) display a striking reactivity on account of their extreme double bond polarization (in C₆D₆, 3 shows a shift of $\delta = 2.77$ ppm for its olefinic protons [21]). This behavior can be explained by the formation of an aromatic imidazolium moiety once charge separation occurs for NHOs such as 3 or 6 (see also Figure 1b). Reports consequently describe a very different behavior in organopolymerization, where imidazole-based NHOs frequently are able to polymerize while the saturated analogues remain inactive, as was found for lactones, epoxides or acrylic monomers [14,31,35]. The increased electron density on the exocyclic carbon should therefore render NHO 3 most prone for coordination to a Lewis acid, a conclusion that is supported by the data listed in Tables 1 and 2; the ZnCl₂(3)(THF) adduct accounts for the most exothermic reaction energy for all investigated NHO/metal halide combinations (−53.4 kJ/mol). The series 4–6, analogous to 1–3 but with additional dimethyl-substitution on the exocyclic carbon (C=C(CH₃)₂ moiety) is of significance since this modification is a prerequisite for successful polymerization in lactone or even acrylate polymerization [31,35]. This also shows in the binding propensity, which is in all three cases much less pronounced than for the non-substituted compounds. For 4 and 5 (MgCl₂, ZnCl₂) the reaction energies even turn endothermic, while for the imidazole-derivative 6 still a negative free reaction energy was calculated. Obviously, the increased steric congestion disfavors adduct formation (see Table 4 for buried volumes, %V_{Bur}, of NHOs 1–8) [36,37]. Since compounds 4–6 have been highly successful in the Lewis pair polymerization of lactones [11,12], including the polymerization of VL, CL and PDL as well as the copolymerization of GBL, this destabilization of adducts seems to be beneficial for catalytic activity. Moving to compound 7, a benzimidazole derivative, the data from MgCl₂ and ZnCl₂ coordination put this NHO in an intermediate range between the less polarized saturated ring systems and the imidazole structure 6. This suggests that benzimidazole backbones might be suitable to realize polymerization systems where the NHO is still considerably active, but does not form too strongly associated Lewis pairs. Experimental data for this NHO is scarce, but a report on VL/CL homo- and copolymerization (in cooperation with Lewis acids such as MgCl₂, ZnCl₂, YCl₃) attests to a high catalytic performance with good control over polydispersity ($D_M = 1.1$) [11]. Finally, NHO 8 shall be considered. For this saturated, five-membered compound a seemingly small change (connecting the exocyclic methyl substituents to form a cyclopropane) can be observed to have a surprising impact. Comparing the reaction energies for 1, 4, and 8 (ZnCl₂) of −26.6 kJ/mol, +7.6 kJ/mol and −44.1 kJ/mol, respectively, reveals that the bonding propensity for this particular NHO is the strongest in this series and even more pronounced than for imidazole derivative 6 (for MgCl₂ the same applies). This is striking; potentially, the electron donating effect exerted by the cyclopropane moiety overcompensates for steric crowding (according to Table 4 the steric demand of 8 is intermediate between NHOs 1 and 4) and for having a saturated backbone in the heterocyclic ring. ¹³C-NMR investigations of this compound attest to the high electron density on the exocyclic, olefinic carbon [20], which can be interpreted to support the calculated propensity for complex formation. Information on the polymerization activity of this NHO does currently not exist, but a high activity in organopolymerization might be expected on the basis of these findings.

Table 4. Buried volume as calculated for MgCl₂(NHO)(THF) [38].

NHO	1	2	3	4	5	6	7	8
%V _{Bur}	23.4	23.1	22.7	30.5	31.6	29.7	30.2	26.6

Overall, the results described in this section indicate that adduct formation for NHO/metal halides Lewis pairs can be readily influenced—perhaps even tailored—by suitable selection of both components. For example, the 4/LiCl LP can be expected to offer a high degree of “free” cocatalysts, while the application of 3/ZnCl₂ should provide a result from the other end of the scale. Furthermore, it was found that the exocyclic substituents are a prime tuning site for regulating adduct formation. The good congruency of experimental findings with the tendencies described in this section also suggest that future NHO (co)catalysts could be conveniently screened in this manner, with a limited computational effort (see Computational Details).

2.2. Coordination of Lactones to MgCl₂

Another central assumption in the discussed type of LP lactone polymerization is the activation of the monomer by the Lewis acid. As a representative example we have chosen MgCl₂ and studied its interaction with β-butyrolactone (BBL), GBL, VL and CL in different coordination geometries and activation modes (Figure 2). The coordination geometries include (distorted) tetrahedral and trigonal-bipyramidal configurations, while the activation modes include lactone-metal interactions via the endocyclic oxygen, via the carbonyl oxygen and a chelating binding motif employing both oxygens. By choice of the authors, octahedral complexes were not considered; the similar, although not identical, situation with NHC-MgCl₂ complexes suggested low coordination numbers [4]. For all models it was assumed that the Mg-Cl bonds remain intact and free coordination space is taken up by THF (one solvent molecule for the tetrahedral coordination, two THF molecules for trigonal-bipyramidal configuration). Interaction of the lactone with MgCl₂ in the pentacoordinate scenario always resulted in the apical positioning of the monomer being preferred.

For the optimized structures, results are given in Tables 5 and 6. The distances of Mg to the relevant oxygen atoms are listed, whereby d_3 and d_4 describe the distance to the endocyclic and carbonyl oxygen, respectively. For VL and CL, no minimum structure for the endocyclic binding motif could be found in case of the tetrahedral [MgCl₂(Lactone)(THF)] complex. All attempts to identify this local minimum resulted in the bidentate structure. This implies, before any quantitative evaluation is considered, that the endocyclic type of activation is energetically disfavored. Likewise, no minimum structure for this coordination was obtained for VL and GBL in the trigonal-bipyramidal configuration, i.e., [MgCl₂(Lactone)(THF)₂].

Table 5. Distances between magnesium and relevant oxygen atoms of the coordinated lactones in the tetrahedral [MgCl₂(Lac)(THF)] structures. Data in (Å).

Lactone	d_3			d_4			
	Binding Mode	Endocycl.	Carbonyl	Bidentate	Endocycl.	Carbonyl	Bidentate
BBL		2.16	4.26	3.45	3.67	2.08	2.10
GBL		2.17	4.21	3.22	3.43	2.07	2.09
VL		-	4.17	2.96	-	2.05	2.09
CL		-	4.18	2.79	-	2.05	2.10

Table 6. Distances between magnesium and relevant oxygen atoms of the coordinated lactones in the trigonal-bipyramidal [MgCl₂(Lac)(THF)₂] structures. Data in (Å).

Lactone	d_3			d_4			
	Binding Mode	Endocycl.	Carbonyl	Bidentate	Endocycl.	Carbonyl	Bidentate
BBL		2.39	4.43	3.47	3.94	2.24	2.22
GBL		-	4.31	3.30	-	2.17	2.19
VL		-	4.30	3.10	-	2.16	2.17
CL		2.64	4.29	3.10	3.54	2.15	2.18

Noticeably, the distances between magnesium and the oxygen atoms are slightly longer for the four-membered BBL, compared to other lactones. This suggests weaker binding to Mg^{2+} , an assumption that is also mirrored by the corresponding ΔG_R values (see below). Generally, for all lactones the O–Mg distances are larger in the trigonal-bipyramidal coordination, which most probably reflects the increased steric hindrance caused by the fifth ligand. Interestingly, also a preference for certain binding motifs becomes apparent. Coordination via the endocyclic oxygen alone is clearly disfavored. Even where such species were identified, d_3 is relatively long with 2.16–2.17 Å (tetrahedral) and 2.39–2.64 Å (trigonal-bipyramidal). For comparison, the bond length to THF in these complexes is 2.08 Å and 2.10/2.20 (equatorial/apical), respectively. This implies a rather weak bonding, which is potentially caused by the reduced electron density on this oxygen atom compared to its carbonyl counterpart and the steric demand exerted by the neighboring carbonyl group, impairing coordination (see bottom left structure, Figure 2). For the bidentate activation mode, only rather high d_3 values were found (2.79–3.45 Å, 3.10–3.47 Å), while the distance to the carbonyl oxygen (d_4) was in the range of 2.09–2.10 Å and 2.17–2.22 Å, respectively, for the two geometries investigated. While this negates a truly chelating coordination of the lactone, it is nonetheless interesting to note that the Mg–O (d_3) interaction significantly grows upon increasing the ring size of the monomer, as evidenced by the shrinking interatomic distances reported in Tables 5 and 6.

The most probable explanation for this behavior is found in the required four-membered cycle (Mg–O–C–O), which is clearly strained. However, this strain lessens when the O–C–O angle gets smaller; consequently, for BBL with its rigid structure and largest O–C–O angle an effective bidentate activation is clearly disfavored, while CL with its smaller corresponding angle and higher flexibility can achieve a distance d_3 of 2.79 Å, indicating a weak interaction. The third mode of activation, exclusively via the carbonyl oxygen, delivers the shortest Mg–O distances of all investigated binding motifs, suggesting it as the preferred coordination type for the lactone. This is also supported by another indicator for the strength of the binding of the lactones to magnesium, namely the binding energy derived from the Gibbs Free Energy of the reaction [39–41]:



Geometries as depicted in Figure 2 were employed. The results of these calculations are summarized in Table 7.

Table 7. Reaction energies (ΔG_R) for the substitution of a THF molecule by a lactone. Data in (kJ/mol).

Lactone	Tetrahedral Complex			Trigonal Bipyramidal Compl.			
	Binding Mode	Endocycl.	Carbonyl	Bidentate	Endocycl.	Carbonyl	Bidentate
BBL		+15.1	+6.6	+10.7	+28.0	+25.5	+28.8
GBL		+16.9	−0.4	+1.5	-	−8.3	+4.6
VL		-	−6.6	−7.8	-	−0.6	+2.9
CL		-	+12.5	+7.1	+13.1	−0.1	−5.1

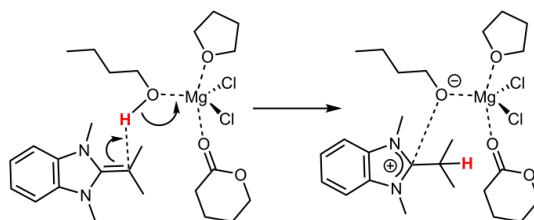
The Gibbs Free Energy of the reaction for BBL is generally higher than the corresponding data of the other lactones, implying that BBL is less likely bound and thereby also less likely to be activated for ring-opening in this manner. Albeit circumstantial, it is still noteworthy that so far no reports for BBL polymerization using this type of LP exist, perhaps a consequence of the seemingly ineffectual activation.

For all lactones, the endocyclic binding mode displays a rather large average reaction energy of +18.3 kJ/mol. Together with the findings on Mg–O bond lengths (see above) this suggests that this mode of coordination can be considered less likely. For the bidentate binding mode, the average reaction energy (+5.3 kJ/mol) is slightly higher than the average reaction energy of the carbonyl-only motif (+3.6 kJ/mol), thus the latter type of activation is again rendered the most favored one.

Hence, overall an endocyclic-only coordination can be discounted, while activation via the carbonyl is most likely. Tentatively, this can be correlated with experimental observations. A $YCl_3(CL)_3$ complex has been characterized by crystal data analysis [42], whereby all three CL ligands in this complex are exclusively coordinated via the carbonyl oxygen. However, it is unclear whether the same applies in solution. A chelate-like coordination by the lactone cannot be ruled out by the results discussed above. The stepwise increasing ability of the lactone to achieve coordination via both oxygen species as the ring size grows from the four-membered BBL to the seven-membered CL (especially tetrahedral coordination, see Table 5) could indicate that this is one of the mechanisms by which monomer selectivity is engendered in the NHO/metal halide LP polymerization setup.

2.3. Initiation: Proton Transfer Step

Finally, the initial step of the polymerization process, which is often described as the deprotonation/activation of an initiating alcohol species, was also investigated. As model components, the interaction of $MgCl_2$ with one VL and one THF molecule in the presence of butanol was investigated. As NHO compound 7 was selected (Scheme 3, Figure 3), since this structure represents intermediate polarization. Also, the successful polymerization of VL by 7/ $MgCl_2$ has been reported in the presence of an alcohol as initiator (conversion > 90%, 80 min, 1% NHO-loading, $D_M = 1.10$ – 1.20) [11].



Scheme 3. Model employed for calculation of the proton transfer.

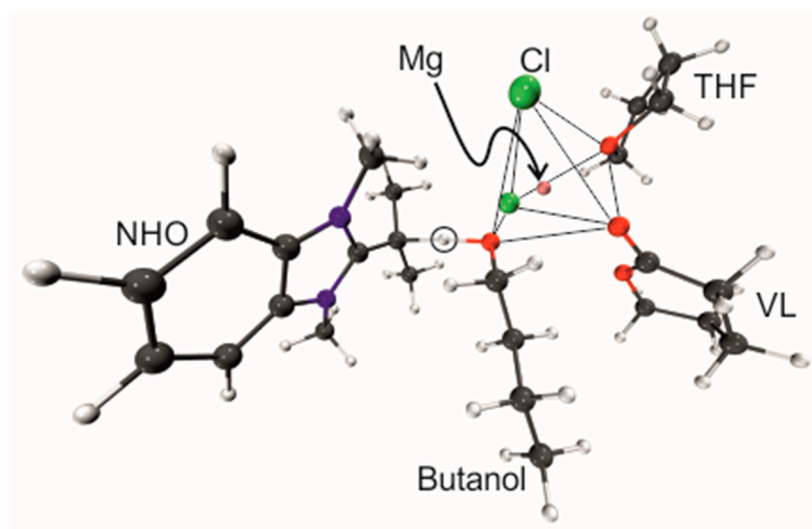


Figure 3. Transition structure of the proton transfer. The lines indicate the trigonal-bipyramidal coordination polyhedron. Encircled: Transferred proton.

Calculations revealed a potential activation energy barrier of 30.2 kJ/mol for the proton transfer (20.9 kJ/mol including zero point energy (ZPE)) and a potential reaction energy of -14.5 kJ/mol (-13.3 kJ/mol including ZPE), rendering this process well feasible. However, *without* $MgCl_2$ being present, the deprotonation of butanol with NHO 7 was calculated to be endothermic by approximately 65 kJ/mol (see also Figure S1, Supplementary Materials). Significantly, this is in accordance with

recent experimental descriptions of the deprotonation of benzyl alcohol, a typical initiator for lactone polymerization, where it was detailed that in the absence of metal-based Lewis acids no proton transfer was observed ($^1\text{H-NMR}$), yet with different metal halides varying proportions of protonated NHO species were detected [12]. Thus, especially less reactive NHOs (such as **1**, **2**, **4**, **5** or **7**) seem to require the additional support by a Lewis acid to efficiently polymerize lactones, most probably because the electron deficient metal species stabilizes the formation of an oxyanionic species (butanolate) from the initiator and thus acidifies the $-\text{OH}$ functional group.

During the course of the proton transfer the coordination sphere of Mg^{2+} remains broadly unchanged. The $\text{Mg-O}_{\text{butanol}}$ distance (Table 8) shrinks from 2.13 Å to 1.95 Å, nicely mirroring the stronger bonding of the butanolate to Mg^{2+} (as compared to the initial butanol). The olefinic $\text{C}=\text{C}$ double bond in the NHO is converted into a single bond upon protonation, which is reflected by the changing $\text{C}-\text{C}$ distance, growing from 1.39 Å to 1.50 Å.

Table 8. Relevant interatomic distances changing during the proton transfer step. All values in (Å).

Parameter	Alcohol Coordinated	Deprotonated
$d(\text{O}_{\text{butanol}}-\text{H})$	1.01	1.92
$d(\text{C}_{\text{NHO}}-\text{H})$	1.98	1.13
$d(\text{Mg}-\text{O}_{\text{butanol}})$	2.13	1.95
$d(\text{C}=\text{C})$	1.39	1.50

3. Computational Details

All density functional calculations were carried out using Turbomole v. 7.0.1 [44]. Geometry optimizations have been performed using the dl-find optimization library interfaced via ChemShell with default convergence criteria [45]. For geometry optimizations, the BP-86 functional [46–50] in combination with the def2-SVPD basis set [51] was used throughout. To account for the solvation, which is crucial for the stabilization of the partial charges occurring, i.e., for the adduct formation and the proton transfer reaction, the Conductor-like Screening Model (COSMO) [52] with the dielectric constant of $\epsilon(\text{THF}) = 7.58$ was applied in these cases (Sections 2.1 and 2.3). To improve the quality of the potential energy, single point calculations using the M06-2X functional [53] in combination with the def2-TZVPD basis set have been performed on all structures, as this functional was shown to perform well [54,55]. Test calculations showed that for the adduct formation of NHO **1** to MgCl_2 (see Scheme 2) the potential reaction energy of 13.2 kJ/mol obtained at M06-2X/def2-TZVPD//M06-2X/def2-SVPD level deviates just slightly from the potential reaction energy of 14.2 kJ/mol obtained by M06-2X/def2-TZVPD//MP86/def2-SVPD. All self-consistent field (SCF) cycles were iterated until the electronic energies changed by less than 10^{-9} Hartree between two successive iterations. The m5 multi-grid was used [56]. Zero point energies and thermal corrections were calculated in the approximation of harmonic oscillators at 300 K. In Sections 2.1 and 2.2, Gibbs Free Energies are given and in Section 2.3 sole potential energies (on M06-2X/def2-TZVPD level) are provided.

4. Conclusions

Adduct formation, a major factor in Lewis pair polymerization, has been shown to be readily tunable in the case of NHO/metal halide co-catalysts. Among the three investigated Lewis acids, the bonding propensity is strongest for ZnCl_2 , followed by MgCl_2 and LiCl , with the latter displaying only a weak interaction. In the same order the formation of true end-on coordination recedes. The ability to efficiently form adducts can also be influenced on the NHO side. In general, saturated NHO backbones reduce the polarization of the olefinic bond and likewise disfavor adduct formation. Similarly, the introduction of substituents on the exocyclic olefinic carbon can destabilize NHO/metal halide complexes on account of the increased steric congestion.

Lactone activation via coordination to a Lewis acid is a key motif for many proposed LP polymerization mechanisms. According to the findings presented in this work, if this coordination occurs it will most likely happen via the carbonyl oxygen. An endocyclic-only coordination can be ruled out. Interaction via both oxygen species in the lactone seems to gain importance for the larger-ring monomers, potentially suggesting one possible mode by which monomer selectivity is generated.

The presence of a metal species also influences the acid-base behavior of NHO and alcohol-based initiators. NHOs of only intermediate polarization cannot deprotonate –OH functionalities in a metal-free setup. As detailed for 7/MgCl₂, this changes in the presence of the Lewis acid, where then a well feasible, exothermic process with a low barrier could be identified. These observations are in accordance with the (limited) experimental data available so far, suggesting that the computational evaluation of NHO/metal halide pairs can usefully complement experimental screenings.

Supplementary Materials: The following are available online. molecular coordinates for various structures, TAR-archive for DFT structures, Figure S1: Proton transfer in the absence of MgCl₂.

Acknowledgments: Stefan Naumann gratefully acknowledges funding by the German Research Foundation (DFG, NA 1206-2). DFG support within the Cluster of Excellence in Simulation Technology (EXC 310/2) at the University of Stuttgart is also acknowledged. Prof. Dietrich Gudat (University of Stuttgart) is thanked for helpful discussions.

Author Contributions: All authors jointly conceived and designed the computations; J.M. and J.K. performed the calculations; J.M., S.N. and J.K. analyzed the data; J.M., S.N. and J.K. wrote the paper.

Conflicts of Interest: The authors declare no conflict of interest.

References and Notes

1. Zhang, Y.; Miyake, G.M.; John, M.G.; Falivene, L.; Caporaso, L.; Cavallo, L.; Chen, E.Y.-X. Lewis pair polymerization by classical and frustrated Lewis pairs: Acid, base and monomer scope and polymerization mechanism. *Dalton Trans.* **2012**, *41*, 9119–9134. [[CrossRef](#)] [[PubMed](#)]
2. Piedra-Arroni, E.; Amgoune, A.; Bourissou, D. Dual catalysis: New approaches for the polymerization of lactones and polar olefins. *Dalton Trans.* **2013**, *42*, 9024–9029. [[CrossRef](#)] [[PubMed](#)]
3. Piedra-Arroni, E.; Ladavière, C.; Amgoune, A.; Bourissou, D. Ring-Opening Polymerization with Zn(C₆F₅)₂-Based Lewis Pairs: Original and Efficient Approach to Cyclic Polyesters. *J. Am. Chem. Soc.* **2013**, *135*, 13306–13309. [[CrossRef](#)] [[PubMed](#)]
4. Naumann, S.; Schmidt, F.G.; Frey, W.; Buchmeiser, M.R. Protected *N*-heterocyclic carbenes as latent pre-catalysts for the polymerization of ϵ -caprolactone. *Polym. Chem.* **2013**, *4*, 4172–4181. [[CrossRef](#)]
5. Jia, Y.-B.; Wang, Y.-B.; Ren, W.-M.; Xu, T.; Wang, J.; Lu, X.-B. Mechanistic Aspects of Initiation and Deactivation in *N*-Heterocyclic Olefin Mediated Polymerization of Acrylates with Alane as Activator. *Macromolecules* **2014**, *47*, 1966–1972. [[CrossRef](#)]
6. Knaus, M.G.M.; Giuman, M.M.; Pothig, A.; Rieger, B. End of Frustration: Catalytic Precision Polymerization with Highly Interacting Lewis Pairs. *J. Am. Chem. Soc.* **2016**, *138*, 7776–7781. [[CrossRef](#)] [[PubMed](#)]
7. Nzahou Ottou, W.; Conde-Mendizabal, E.; Pascual, A.; Wirotius, A.-L.; Bourichon, D.; Vignolle, J.; Robert, F.; Landais, Y.; Sotiropoulos, J.-M.; Miqueu, K.; et al. Organic Lewis Pairs Based on Phosphine and Electrophilic Silane for the Direct and Controlled Polymerization of Methyl Methacrylate: Experimental and Theoretical Investigations. *Macromolecules* **2017**, *50*, 762–774. [[CrossRef](#)]
8. Wang, Q.; Zhao, W.; He, J.; Zhang, Y.; Chen, E.Y.-X. Living Ring-Opening Polymerization of Lactones by *N*-Heterocyclic Olefin/Al(C₆F₅)₃ Lewis Pairs: Structures of Intermediates, Kinetics, and Mechanism. *Macromolecules* **2017**, *50*, 123–136. [[CrossRef](#)]
9. Ji, H.-Y.; Wang, B.; Pan, L.; Li, Y.-S. Lewis pairs for ring-opening alternating copolymerization of cyclic anhydrides and epoxides. *Green Chem.* **2018**, *20*, 641–648. [[CrossRef](#)]
10. Naumann, S.; Scholten, P.B.V.; Wilson, J.A.; Dove, A.P. Dual Catalysis for Selective Ring-Opening Polymerization of Lactones: Evolution toward Simplicity. *J. Am. Chem. Soc.* **2015**, *137*, 14439–14445. [[CrossRef](#)] [[PubMed](#)]
11. Naumann, S.; Wang, D. Dual Catalysis Based on *N*-Heterocyclic Olefins for the Copolymerization of Lactones: High Performance and Tunable Selectivity. *Macromolecules* **2016**, *49*, 8869–8878. [[CrossRef](#)]

12. Walther, P.; Naumann, S. *N*-Heterocyclic Olefin-Based (Co)polymerization of a Challenging Monomer: Homopolymerization of ω -Pentadecalactone and Its Copolymers with γ -Butyrolactone, δ -Valerolactone, and ϵ -Caprolactone. *Macromolecules* **2017**, *50*, 8406–8416. [[CrossRef](#)]
13. Fürstner, A.; Alcarazo, M.; Goddard, R.; Lehmann, C.W. Coordination chemistry of Ene-1,1-diamines and a prototype “carbodicarbene”. *Angew. Chem. Int. Ed.* **2008**, *47*, 3210–3214. [[CrossRef](#)] [[PubMed](#)]
14. Naumann, S.; Thomas, A.W.; Dove, A.P. *N*-Heterocyclic Olefins as Organocatalysts for Polymerization: Preparation of Well-Defined Poly(propylene oxide). *Angew. Chem. Int. Ed.* **2015**, *54*, 9550–9554. [[CrossRef](#)] [[PubMed](#)]
15. Crocker, R.D.; Nguyen, T.V. The Resurgence of the Highly Ylidic *N*-Heterocyclic Olefins as a New Class of Organocatalysts. *Chem. Eur. J.* **2016**, *22*, 2208–2213. [[CrossRef](#)] [[PubMed](#)]
16. Blümel, M.; Noy, J.-M.; Enders, D.; Stenzel, M.H.; Nguyen, T.V. Development and Applications of Transesterification Reactions Catalyzed by *N*-Heterocyclic Olefins. *Org. Lett.* **2016**, *18*, 2208–2211. [[CrossRef](#)] [[PubMed](#)]
17. Imbrich, D.A.; Frey, W.; Naumann, S.; Buchmeiser, M.R. Application of imidazolium salts and *N*-heterocyclic olefins for the synthesis of anionic and neutral tungsten imido alkylidene complexes. *Chem. Commun.* **2016**, *52*, 6099–6102. [[CrossRef](#)] [[PubMed](#)]
18. Roy, M.M.D.; Rivard, E. Pushing Chemical Boundaries with *N*-Heterocyclic Olefins (NHOs): From Catalysis to Main Group Element Chemistry. *Acc. Chem. Res.* **2017**, *50*, 2017–2025. [[CrossRef](#)] [[PubMed](#)]
19. Wang, Y.-B.; Wang, Y.-M.; Zhang, W.-Z.; Lu, X.-B. Fast CO₂ sequestration, activation, and catalytic transformation using *N*-heterocyclic olefins. *J. Am. Chem. Soc.* **2013**, *135*, 11996–12003. [[CrossRef](#)] [[PubMed](#)]
20. Gruseck, U.; Heuschmann, M. 2-Alkylidenimidazolidine—Synthese, Basizität, ¹H- und ¹³C-NMR-Spektren. *Chem. Ber.* **1987**, *120*, 2053–2064. [[CrossRef](#)]
21. Kuhn, N.; Bohnen, H.; Kreutzberg, J.; Bläser, D.; Boese, R. 1,3,4,5-Tetramethyl-2-methyleneimidazoline—An Ylidic Olefin. *Chem. Commun.* **1993**, 1136–1137. [[CrossRef](#)]
22. Quast, H.; Ach, M.; Kindermann, M.K.; Rademacher, P.; Schindler, M. Synthese, NMR-Spektren und Photoelektronen-Spektren von cyclischen Keten-*N*,*X*1-acetalen (2-Alkyliden-*N*-heterocyclen). *Chem. Ber.* **1993**, *126*, 503–516. [[CrossRef](#)]
23. Powers, K.; Hering-Junghans, C.; McDonald, R.; Ferguson, M.J.; Rivard, E. Improved synthesis of *N*-heterocyclic olefins and evaluation of their donor strengths. *Polyhedron* **2016**, *108*, 8–14. [[CrossRef](#)]
24. Catoire, A.E.; Beard, D.J.; Saebo, S. Theoretical study of geometry and nucleophilicity of the exocyclic methylene in five-membered ring cyclic ketene acetals, neutral and protonated, containing pnictogen and chalcogen heteroatoms. *Struct. Chem.* **2014**, *25*, 371–376. [[CrossRef](#)]
25. Dong, L.; Wen, J.; Li, W. A theoretical investigation of substituent effects on the stability and reactivity of *N*-heterocyclic olefin carboxylates. *Org. Biomol. Chem.* **2015**, *13*, 8533–8544. [[CrossRef](#)] [[PubMed](#)]
26. Li, W.; Yang, N.; Lyu, Y. Theoretical Insights into the Catalytic Mechanism of *N*-Heterocyclic Olefins in Carboxylative Cyclization of Propargyl Alcohol with CO₂. *J. Org. Chem.* **2016**, *81*, 5303–5313. [[CrossRef](#)] [[PubMed](#)]
27. Li, W.; Huang, D.; Lyu, Y. A comparative computational study of *N*-heterocyclic olefin and *N*-heterocyclic carbene mediated carboxylative cyclization of propargyl alcohols with CO₂. *Org. Biomol. Chem.* **2016**, *14*, 10875–10885. [[CrossRef](#)] [[PubMed](#)]
28. De Lima Batista, A.P.; de Oliveira-Filho, A.G.S.; Galembeck, S.E. Computationally Designed 1,2,4-Triazolylidene-Derived *N*-Heterocyclic Olefins for CO₂ Capture, Activation, and Storage. *ACS Omega* **2017**, *2*, 299–307. [[CrossRef](#)]
29. De Lima Batista, A.P.; de Oliveira-Filho, A.G.S.; Galembeck, S.E. CO₂ Sequestration by Triazolylidene-Derived *N*-Heterocyclic Olefins: A Computational Study. *ChemistrySelect* **2017**, *2*, 4648–4654. [[CrossRef](#)]
30. Al Ghamdi, M.; Cavallo, L.; Falivene, L. Mechanism of Propylene Oxide Polymerization Promoted by *N*-Heterocyclic Olefins. *J. Phys. Chem. C* **2017**, *121*, 2730–2737. [[CrossRef](#)]
31. Naumann, S.; Mundsinger, K.; Cavallo, L.; Falivene, L. *N*-Heterocyclic olefins as initiators for the polymerization of (meth)acrylic monomers: A combined experimental and theoretical approach. *Polym. Chem.* **2017**, *8*, 5803–5812. [[CrossRef](#)]

32. Naumann, S.; Buchmeiser, M.R. Liberation of *N*-heterocyclic carbenes (NHCs) from thermally labile progenitors: Protected NHCs as versatile tools in organo- and polymerization catalysis. *Catal. Sci. Technol.* **2014**, *4*, 2466–2479. [CrossRef]
33. Kronig, S.; Jones, P.G.; Tamm, M. Preparation of 2-Alkylidene-Substituted 1,3,4,5-Tetramethylimidazolines and Their Reactivity Towards Rh^I Complexes and B(C₆F₅)₃. *Eur. J. Inorg. Chem.* **2013**, *2013*, 2301–2314. [CrossRef]
34. Ye, G.; Chatterjee, S.; Li, M.; Zhou, A.; Song, Y.; Barker, B.L.; Chen, C.; Beard, D.J.; Henry, W.P.; Pittman, C.U. Push–pull alkenes from cyclic ketene-*N,N'*-acetals: A wide span of double bond lengths and twist angles: A wide span of double bond lengths and twist angles. *Tetrahedron* **2010**, *66*, 2919–2927. [CrossRef]
35. Naumann, S.; Thomas, A.W.; Dove, A.P. Highly Polarized Alkenes as Organocatalysts for the Polymerization of Lactones and Trimethylene Carbonate. *ACS Macro Lett.* **2016**, *5*, 134–138. [CrossRef]
36. Poater, A.; Cosenza, B.; Correa, A.; Giudice, S.; Ragone, F.; Scarano, V.; Cavallo, L. SambVca: A Web Application for the Calculation of the Buried Volume of *N*-Heterocyclic Carbene Ligands. *Eur. J. Inorg. Chem.* **2009**, *2009*, 1759–1766. [CrossRef]
37. Falivene, L.; Credendino, R.; Poater, A.; Petta, A.; Serra, L.; Oliva, R.; Scarano, V.; Cavallo, L. SambVca 2. A Web Tool for Analyzing Catalytic Pockets with Topographic Steric Maps. *Organometallics* **2016**, *35*, 2286–2293. [CrossRef]
38. Falivene, L.; Credendino, R.; Poater, A.; Petta, A.; Serra, L.; Oliva, R.; Scarano, V.; Cavallo, L. SambVca 2.0. Available online: <https://www.molnac.unisa.it/OMtools/sambvca2.0/index.html> (accessed on 2 February 2018).
39. As pointed out by an observant referee, the entropy is not totally conserved in this reaction as a solvent molecule is released into the same solvent. The entropic contribution to account for the reduced entropy in solution was not scaled. Thus, the absolute reaction free energies might be off, but relative trends, which are of central interest here, should be well preserved. For the problem of scaling entropy contributions in solution (Ref 40) and the problem of estimating entropy contributions if solvent molecules are displaced (Ref 41).
40. Tobisch, S.; Ziegler, T. Catalytic oligomerization of ethylene to higher linear alpha-olefins promoted by the cationic group 4 [(η⁵-Cp-(CMe₂-bridge)-Ph)M^{II}(ethylene)₂]⁺ (M = Ti, Zr, Hf) active catalysts: A density functional investigation of the influence of the metal on the catalytic activity and selectivity. *J. Am. Chem. Soc.* **2004**, *126*, 9059–9071. [PubMed]
41. Ehm, C.; Cipullo, R.; Budzelaar, P.H.M.; Busico, V. Role(s) of TMA in polymerization. *Dalton Trans.* **2016**, *45*, 6847–6855. [CrossRef] [PubMed]
42. Evans, W.J.; Shreeve, J.L.; Doedens, R.J. Isolation and Crystal Structure of a Six Coordinate Yttrium Trichloride Complex of ε-Caprolactone, YCl₃(C₆H₁₀O₂)₃. *Inorg. Chem.* **1993**, *32*, 245–246. [CrossRef]
43. Ahlrichs, R.; Bär, M.; Häser, M.; Horn, H.; Kölmel, C. Electronic structure calculations on workstation computers: The program system turbomole. *Chem. Phys. Lett.* **1989**, *162*, 165–169. [CrossRef]
44. TURBOMOLE V7.0.1 2015, a development of University of Karlsruhe and Forschungszentrum Karlsruhe GmbH, 1989–2007, TURBOMOLE GmbH, since 2007. Available online: <http://www.turbomole.com> (accessed on 20 December 2017).
45. Metz, S.; Kästner, J.; Sokol, A.A.; Keal, T.W.; Sherwood, P. ChemShell—A modular software package for QM/MM simulations. *WIREs Comput. Mol. Sci.* **2014**, *4*, 101–110. [CrossRef]
46. Dirac, P.A.M. Quantum Mechanics of Many-Electron Systems. *Proc. R. Soc. A Math. Phys. Eng. Sci.* **1929**, *123*, 714–733. [CrossRef]
47. Slater, J.C. A Simplification of the Hartree-Fock Method. *Phys. Rev.* **1951**, *81*, 385–390. [CrossRef]
48. Vosko, S.H.; Wilk, L.; Nusair, M. Accurate spin-dependent electron liquid correlation energies for local spin density calculations: A critical analysis. *Can. J. Phys.* **1980**, *58*, 1200–1211. [CrossRef]
49. Perdew, J.P. Density-functional approximation for the correlation energy of the inhomogeneous electron gas. *Phys. Rev. B* **1986**, *33*, 8822–8824. [CrossRef]
50. Becke, A.D. Density-functional exchange-energy approximation with correct asymptotic behavior. *Phys. Rev. A* **1988**, *38*, 3098–3100. [CrossRef]
51. Rappoport, D.; Furche, F. Property-optimized gaussian basis sets for molecular response calculations. *J. Chem. Phys.* **2010**, *133*, 134105. [CrossRef] [PubMed]
52. Klamt, A.; Schüürmann, G. COSMO: A new approach to dielectric screening in solvents with explicit expressions for the screening energy and its gradient. *J. Chem. Soc. Perkin Trans. 2* **1993**, 799–805. [CrossRef]

53. Zhao, Y.; Truhlar, D.G. The M06 suite of density functionals for main group thermochemistry, thermochemical kinetics, noncovalent interactions, excited states, and transition elements: Two new functionals and systematic testing of four M06-class functionals and 12 other functionals. *Theor. Chem. Acc.* **2008**, *120*, 215–241.
54. Miranda, M.O.; DePorre, Y.; Vazquez-Lima, H.; Johnson, M.A.; Marell, D.J.; Cramer, C.J.; Tolman, W.B. Understanding the mechanism of polymerization of ϵ -caprolactone catalyzed by aluminum salen complexes. *Inorg. Chem.* **2013**, *52*, 13692–13701. [[CrossRef](#)] [[PubMed](#)]
55. Chandanabodhi, D.; Nanok, T. A DFT study of the ring-opening polymerization mechanism of L-lactide and ϵ -caprolactone using aluminium salen-type initiators: Towards an understanding of their reactivities in homo- and copolymerization. *Mol. Catal.* **2017**, *436*, 145–156. [[CrossRef](#)]
56. Eichkorn, K.; Weigend, F.; Treutler, O.; Ahlrichs, R. Auxiliary basis sets for main row atoms and transition metals and their use to approximate Coulomb potentials. *Theor. Chem. Acc.* **1997**, *97*, 119–124. [[CrossRef](#)]

Sample Availability: not available.



© 2018 by the authors. Licensee MDPI, Basel, Switzerland. This article is an open access article distributed under the terms and conditions of the Creative Commons Attribution (CC BY) license (<http://creativecommons.org/licenses/by/4.0/>).